Journal of Petroleum Science and Engineering 73 (2010) 99–106

Contents lists available at ScienceDirect

Journal of Petroleum Science and Engineering

journal homepage: www.elsevier.com/locate/petrol

An element-based finite-volume method approach for heterogeneous and anisotropic compositional reservoir simulation

Francisco Marcondes [a], Kamy Sepehrnoori [b,*]

[a] Department of Metallurgical Engineering and Material Science, Federal University of Ceará, Fortaleza, Ceará, Brazil
[b] Petroleum and Geosystems Engineering Department, The University of Texas at Austin, 1 University Station C0300, Austin, TX 78712-0228, USA

ARTICLE INFO

Article history:
Received 30 January 2009
Accepted 15 May 2010

Keywords:
unstructured grids
compositional reservoir
element-based finite-volume method

ABSTRACT

An element-based finite-volume approach in conjunction with unstructured grids for heterogeneous and anisotropic compositional simulation is presented. This approach adds flexibility to map complex features of the reservoir such as irregular boundaries, discrete fractures, faults, inclined and distorted wells. The mesh, for two dimensional domains, can be built of triangles, quadrilaterals or a mix of these elements. According to the number of vertex, each element is divided into sub-elements and then mass balance equations for each component are integrated along each interface of these sub-elements. The finite-volume conservation equations are assembled from the contribution of all the elements that share a vertex creating a cell vertex approach. The results for several compositional reservoir simulation case studies are presented to demonstrate the application of the method.

1. Introduction

Unstructured meshes present an important step in reservoir simulation since there is no line or surface restriction similar to that found in structured meshes. Unstructured meshes based on the finite-volume method have been used for a long time in petroleum reservoir simulation (Forsyth, 1990; Fung et al., 1991; Gottardi and Dall´Olio, 1992; Verma and Aziz, 1997; Edwards, 2000, 2002; Prévost et al., 2002). Also, several authors have employed the finite-element or the mixed finite element methods for solving such problems (Hegre et al., 1986; Durlofsky and Chien, 1993; Deb et al., 1995; Hoteit and Firoozabadi, 2005; Hoteit and Firoozabadi, 2006).

The approach used by Forsyth (1990), Fung et al. (1991) and Gottardi and Dall'Olio (1992) in petroleum reservoir simulation and computational fluid dynamics literature is called Control Volume-based Finite Element Method (CVFEM). In most CVFEM approaches used in petroleum reservoir simulation, the approximate equations for multiphase fluid flow are obtained from the single phase flow and then the transmissibilities are multiplied by the mobilities and densities in order to obtain the equations for the multiphase flow. The approach used by Verma and Aziz (1997), Edwards (2000, 2002), and Prévost et al. (2002) is called multi-point flux approximation (MPFA). In this approach, permeability and porosity are evaluated at the element vertex. In order to calculate the fluxes, along each integration point a local linear system is solved to evaluate the fluxes that obey the flux continuity. Also, in this approach each control volume has a constant porosity and absolute permeability tensor. Using ideas from Raw (1985) and Baliga and Patankar (1983), in conjunction with quadrilateral and triangles, respectively, Cordazzo (2004) and Cordazzo et al. (2004a,b) used a similar approach to the CVFEM methodology to simulate a water flooding problem. However, the approximate equations were obtained using the multiphase equations, rather than obtaining from the approximate equation for single phase flow, and then the transmissibilities were multiplied by the mobilities to obtain the equations for multiphase flow. The authors demonstrated that the equations obtained from a single phase flow do not correctly approximate the equations for multiphase flow. If the approximate equations are obtained for single phase flow and then transmissibilities are multiplied by mobilites in order to obtain the equations for multiphase flow, the angles of meshes must be equal to or less than right angles, in order to avoid negative transmissibilities. This restriction can be difficult to follow for most reservoirs due mainly to the heterogeneity of the medium, fractures, faults, or even generic boundaries of the reservoirs. Cordazzo (2004) and Cordazzo et al. (2004a,b) called their methodology element-based finite-volume method (EbFVM). The term EbFVM seems to be more appropriate than CVFEM used by other authors. As explained by Maliska (2004), we have a methodology that still follows the conservative principles at the discrete level and only borrows the idea of elements and shape functions from the finite element method. Cordazzo (2004) used an Implicit Pressure Explicit Saturation (IMPES) formulation in conjunction with high distorted triangular and quadrilateral elements with EbFVM to simulate two phase fluid flow (oil and water) problems. Excellent results were obtained with very little grid orientation effects.

* Corresponding author. Tel.: +1 512 417 231; fax: +1 512 471 9605.
E-mail address: kamys@mail.utexas.edu (K. Sepehrnoori).

0920-4105/$ – see front matter © 2010 Elsevier B.V. All rights reserved.
doi:10.1016/j.petrol.2010.05.011

Marcondes and Sepehrnoori (2007) applied EbFVM to simulate compositional, multiphase, multi-component fluid-flow problems in conjunction with anisotropic and heterogeneous reservoirs. Although the meshes used for the most of the investigations presented several elements with angles equal or bigger than right angles, the results obtained with triangles and quadrilateral presented a good agreement. In this study, we investigated the EbFVM in conjunction with 2D heterogeneous and anisotropic reservoirs. We expect that most of the findings observed with the unstructured approach presented in the present paper for 2D reservoirs can be extended to 3D reservoirs. Except for absolute permeability tensor and porosity, all the physical parameters are evaluated at the vertices of each element rendering a cell vertex approach. As each element has a constant permeability tensor, all the fluxes along each integration point employ the same absolute permeability. On the other hand, if the permeability tensor is stored in the vertexes of the element an interpolation procedure to evaluate the fluxes along each integration point of each element is necessary, as used in the MPFA approach by Verma and Aziz (1997), Edwards (2000, 2002), and Prévost et al. (2002). The EbFVM was implemented in an in-house compositional simulator called General Purpose Adaptive Simulator (GPAS). GPAS was developed at the Center for Petroleum and Geosystems Engineering at The University of Texas at Austin for the simulation of enhanced recovery processes. GPAS is a fully implicit, multiphase/multi-component simulator which can handle the simulation of several enhanced oil recovery processes. This simulator is divided into two main modules: Framework and EOScomp. Framework is responsible for input/output and memory allocation, while EOScomp handles the computations for flash calculation and solution of non-linear equations arising from the discretization of the governing equations. Details of EOScomp and Framework modules can be found in Wang et al. (1997) and Parashar et al. (1997), respectively.

2. Physical model

Isothermal, multi-component, multiphase fluid flow in a porous medium can be described using three types of equations: the component-material balance equation, phase equilibrium equation, and equation for constraining phase saturations and component concentrations (Wang et al., 1997).

The material balance equation for the i-th component for a full symmetric permeability tensor using the Einstein notation can be written as

$$\frac{\partial(\phi N_i)}{\partial t} - \nabla\cdot\left[\sum_{j=1}^{n_p}\xi_j x_{ij}\lambda_j \;\; \overline{\overline{K}}\cdot\nabla\Phi_j\right] - \frac{q_i}{V_b} = 0; i = 1,2,..,n_c. \tag{1}$$

In Eq. (1), n_c is the number of hydrocarbon components, n_p is the number of phases present in the reservoir, ϕ is the porosity, N_i is the moles of the i-th component per unit of pore volume, ξ_j and λ_j are the molar density and relative mobility of the j-th phase respectively, x_{ij} is the molar fraction of the i-th component in the j-th phase, $\overline{\overline{K}}$ is the absolute permeability tensor, and V_b is a volume of control volume that could contain a well. Φ_j is the potential of the j-th phase and is given by

$$\Phi_j = P_j - \gamma_j Z \tag{2}$$

where P_j denotes the pressure of the j-th phase and Z is depth, which is positive in a downward direction.

The first partial derivative of the total Gibbs free energy with respect to the independent variables gives the equality of component fugacities among all phases,

$$f_i = f_i^j - f_i^r = 0; i = 1,.....,n_c; j = 2,.....,n_p. \tag{3}$$

In Eq. (3), $f_i^j = \ln(x_{ij}\phi_{ij})$, where ϕ_{ij} is the fugacity coefficient of component i in the j-th phase, r denotes the reference phase, and n_c is the number of components excluding the water. The restriction of the molar fraction is used to obtain the solution of Eq. (3),

$$\sum_{i=1}^{n_c} x_{ij} - 1 = 0, j = 2,..,n_p;\ \sum_{i=1}^{n_c}\frac{z_i(K_i-1)}{1+\nu(K_i-1)} = 0 \tag{4}$$

where z_i is the overall molar fraction of the i-th component, K_i is the equilibrium ratio for the i-th component, and ν is the mole fraction of the gas phase in the absence of water. The closure equation comes from the volume constraint, i.e., the available pore volume of each cell must be filled by all phases present in the reservoir. This constraint gives rise to the following equation:

$$V_b\sum_{i=1}^{n_c+1}(\phi N_i)\sum_{j=1}^{n_p} L_j\ \overline{v}_j - V_p = 0 \tag{5}$$

where V_p is the pore volume, and $\overline{v}_j$ is the molar volume of the j-th phase. In GPAS the unknown primary variables are water pressure P_w, N_1,.., N_{nc}, $\ln K_1$,.., $\ln K_{nc}$.

3. Approximate equation

In the EbFVM, each element is divided into sub-elements. These sub-elements will be called sub-control volumes. The conservation equation, Eq. (1), needs to be integrated for each one of these sub-control volumes. Fig. 1 presents a triangular and a quadrilateral element and all of the sub-control volumes associated with each

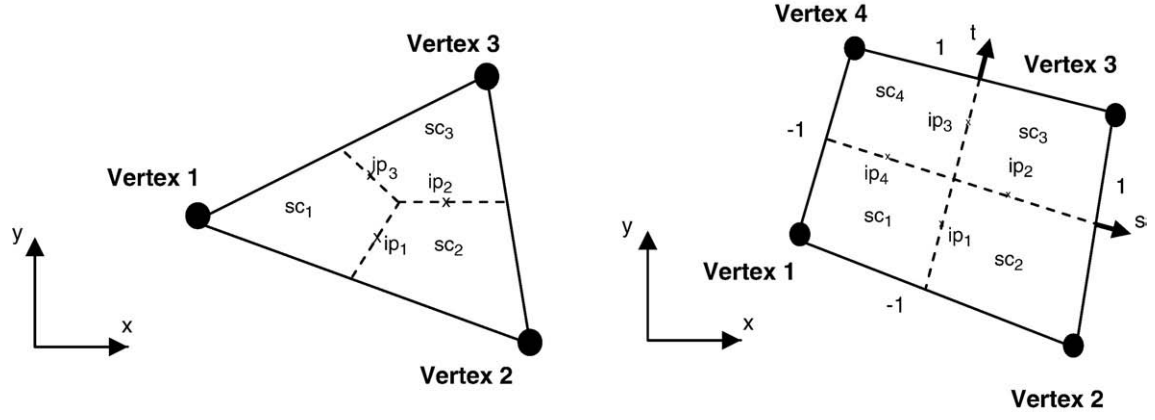

Fig. 1. Triangular and quadrilateral elements and their respective sub-control volumes.

element. Integrating Eq. (1) in time and for each one of the sub-control volumes, and applying the Gauss theorem for the advective term we obtain:

$$\int_V \frac{\partial(\phi N_i)}{\partial t} dV - \int_A \sum_{j=1}^{n_p} \xi_j x_{ij} \lambda_j \overline{\overline{K}} \cdot \nabla \Phi_j \cdot \vec{dA} - \int_V \frac{q_i}{V_b} = 0; i = 1, 2, .., n_c. \quad (6)$$

To evaluate the first and second terms of Eq. (6), it is necessary to define the shape functions. For triangles and quadrilaterals, linear and bi-linear shape functions as defined through Eqs. (7) and (8), will be used, respectively.

$$N_1(s,t) = 1 - s - t;\ N_2(s,t) = s;\ N_3(s,t) = t \quad (7)$$

$$\begin{aligned} &N_1(s,t) = 1/4^*(1-s)(1-t);\ N_2(s,t) = 1/4^*(1+s)(1-t); \\ &N_3(s,t) = 1/4^*(1+s)(1+t);\ N_4(s,t) = 1/4^*(1-s)(1+t). \end{aligned} \quad (8)$$

Using the shape functions any physical properties or positions can be evaluated inside an element as

$$x(s,t) = \sum_{i=1}^{Nv} N_i x_i;\ y(s,t) = \sum_{i=1}^{Nv} N_i y_i;\ \Phi_j(s,t) = \sum_{i=1}^{Nv} N_i \Phi_{ji} \quad (9)$$

where N_v denotes the number of vertex for each element. Elements using the same shape function for coordinates and physical properties are known as isoparametric elements (Hughes, 1987). Using the shape functions, gradients of potentials can be easily evaluated as

$$\frac{\partial \Phi_j}{\partial x} = \sum_{i=1}^{Nv} \frac{\partial N_i}{\partial x} \Phi_{ji};\ \frac{\partial \Phi_j}{\partial y} = \sum_{i=1}^{Nv} \frac{\partial N_i}{\partial y} \Phi_{ji}. \quad (10)$$

To evaluate the gradients, it is necessary to obtain the derivatives of shape functions relative to x and y. These derivatives are given by

$$\frac{\partial N_i}{\partial x} = \frac{1}{\det(J_t)} \left(\frac{\partial N_i}{\partial s}\frac{\partial y}{\partial t} - \frac{\partial N_i}{\partial t}\frac{\partial y}{\partial s} \right);\ \frac{\partial N_i}{\partial y} = \frac{1}{\det(J_t)} \left(\frac{\partial N_i}{\partial t}\frac{\partial x}{\partial s} - \frac{\partial N_i}{\partial s}\frac{\partial x}{\partial t} \right) \quad (11)$$

where J_t is the Jacobian of the transformation and it is given by

$$\det(J_t) = \left(\frac{\partial x}{\partial s}\frac{\partial y}{\partial t} - \frac{\partial x}{\partial t}\frac{\partial y}{\partial s} \right). \quad (12)$$

Further details of the expressions given by Eq. (11) can be found in Maliska (2004) and Cordazzo (2004). To perform the integral of Eq. (6), it is necessary to define the volumes of each sub-control volume and the area of each interface. The volumes of each sub-control for triangles and quadrilaterals, respectively, are given by

$$Vscv_i = \frac{\det(J_t)\Delta s\, \Delta t\, h}{6} \quad (13)$$

$$Vscv_i = \det(J_t)\Delta s\, \Delta t\, h \quad (14)$$

where h is the thickness of the reservoir. For quadrilateral $\det(J_t)$ needs to be evaluated at the center of each sub-control volume. The area of each interface, reading a counterclockwise, is given by

$$\vec{dA} = hdy\,\vec{i} - hdx\,\vec{j}. \quad (15)$$

Substituting Eqs. (13) and (14) for the accumulation term, and Eq. (15) for the advective flux into Eq. (6), and evaluating the fluid properties through a fully implicit procedure the following equations for the two mentioned terms are obtained:

$$Acc_{m,i} = Vscv_{m,i} \left(\left(\frac{\phi N_m}{\Delta t} \right)_i - \left(\frac{\phi N_m}{\Delta t} \right)_i^o \right); m = 1, N_v \quad (16)$$

$$F_{m,i} = \int_A \sum_{j=1}^{n_p} \xi_j x_{ij} \lambda_j \overline{\overline{K}} \cdot \nabla \Phi_j \cdot \vec{dA} = \int_A \sum_{j=1}^{n_p} \xi_j x_{ij} \lambda_j K_{np} \frac{\partial \Phi_j}{\partial x_p} dA_n; \quad m = 1, N_v;\ n, p = 1, 2. \quad (17)$$

By inspecting Eq. (17), it can be inferred that it is necessary to evaluate molar densities, molar fraction and mobilities in two interfaces of each sub-control volume. To evaluate these properties, an upwind scheme based on Cordazzo (2004) will be used. The mobilities and other fluid properties are evaluated at the integration point 1 of Fig. 1, for instance, by

$$\begin{aligned} &\lambda_{j1} = \lambda_{j2} \quad \text{if} \quad \overline{\overline{K}} \cdot \nabla \Phi_j \cdot \vec{dA}|_{ip1} \le 0 \\ &\lambda_{j1} = \lambda_{j1} \quad \text{if} \quad \overline{\overline{K}} \cdot \nabla \Phi_j \cdot \vec{dA}|_{ip1} > 0 \end{aligned}. \quad (18)$$

Inserting Eqs. (16) and (17) into Eq. (6), the following equation for each element is obtained:

$$Acc_{m,i} + F_{m,i} + q_i = 0;\ m = 1, N_v;\ i = 1, n_c + 1. \quad (19)$$

Eq. (19) denotes the conservation for each sub-control volume of each element. Now, it is necessary to assemble the equation of each control volume obtaining the contribution of each sub-control volume that shares the same vertex. This process is similar to the assembling of the stiffness global matrix in the finite element method. Fig. 2 presents a control volume around vertex 5 (dark continuous lines) that will receive contributions from sc1 of element 1, sc3 of element 2, sc4 of element 6, and sc1 of element 7. It is important to mention that each control-volume equation can have different permeabilities and porosities.

4. Test problems

This section presents four simulation case studies using the EbFVM approach. The first two cases studies were used to validate the present formulation with another in-house petroleum reservoir simulator called UTCOMP (Chang et al., 1990). UTCOMP was developed at the Center for Petroleum and Geosystems Engineering at The University of Texas at Austin for the simulation of enhanced recovery processes. UTCOMP is an IMPEC, multiphase/multi-component compositional equation of state simulator which can handle the simulation of several enhanced oil recovery processes. Only Cartesian meshes can be used with UTCOMP. UTCOMP has been validated with several commercial

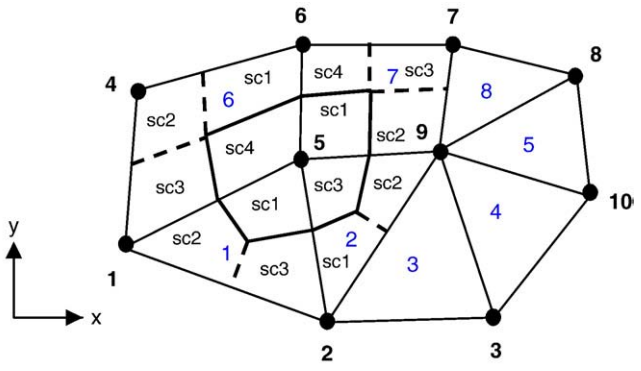

Fig. 2. Control volume.

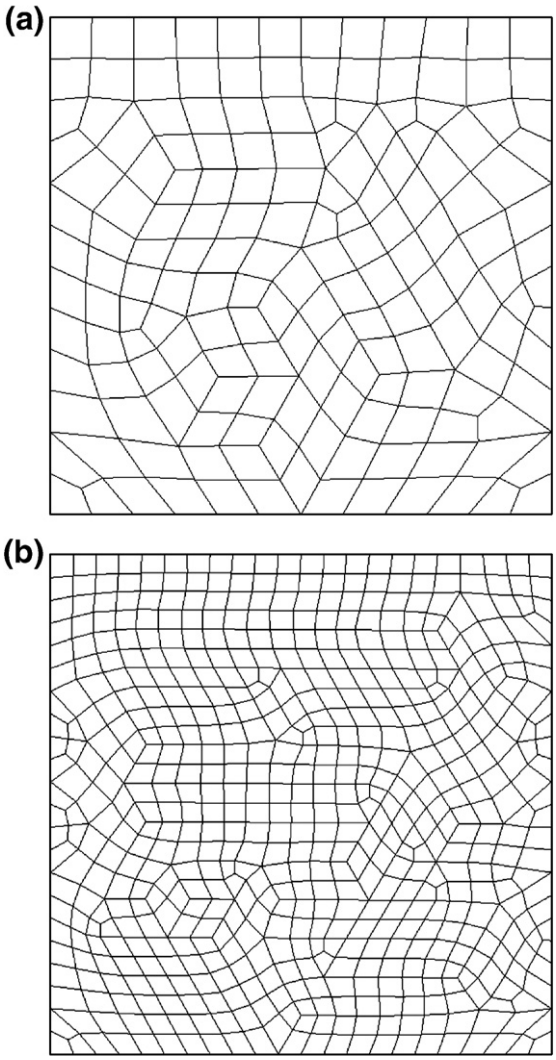

Fig. 3. Quadrilateral-grid configurations used for case studies 1 and 2. a) 195 control volumes and b) 619 control volumes.

codes. Case 1 is the simulation of three-component gas injection in a quarter-of-five spot with the simultaneous flow of gas and oil. Fig. 3 presents the two-grid configurations used for case 1 and case 2. Table 1 presents the fluid and physical properties. The relative permeability data for Corey's model is given in Table 2.

The second case study also refers to gas injection in a quarter-of-five spot, but now the reservoir contains oil that has been characterized using six hydrocarbon components. Except for the initial global molar fraction, all of the previous data presented for case 1 were used. For this case, the components and global molar fractions are the following: C_1 (0.50), C_3 (0.03), C_6 (0.07), C_{10} (0.20), C_{15} (0.15), and C_{20} (0.05).

Table 1
Input data for case 1.

Reservoir data	Initial conditions	Physical properties and well conditions
Reservoir dimension ($L_x = L_y = 170.69$ m, $L_z = 30.48$ m)	Water saturation $S_{wi} = 0.17$	Water viscosity = 1×10^{-3} Pa s
Absolute permeability ($K_{xx} = K_{yy} = K_{zz}$) = 1.0×10^{-14} m^2 (10 mD)	Reservoir pressure = 3.45 MPa (500 psi)	Gas injection rate = 0.164 m^3/s (500×10^3 ft^3/d)
Porosity = 0.35	Overall fraction of hydrocarbon components (C_1, C_3, C_{10}) = 0.3, 0.3, 0.4	Bottom hole pressure = 3.45 MPa (500 psi)

Table 2
Corey's model relative permeability data.

	Water	Oil	Gas
End point relative permeability	1.0	1.0	1.0
Residual saturation	0.2	0.1	0.1
Exponent of relative permeability	1.0	1.0	1.0

The third case study again refers to a gas injection in a quarter-of-five spot and the reservoir fluid again was characterized by the same 3 hydrocarbon components used in case 1, but now the effect of a homogenous and anisotropic tensor is accounted for. For this case, the following values of $\overline{\overline{K}}$ were used: $K_{xx} = K_{yy} = 1.0 \times 10^{-13}$ m^2 (100 mD), $K_{xy} = K_{yx} = 1.0 \times 10^{-14}$ m^2 (10 mD). Instead of Corey's model, we used the Stone II model for the relative permeabilities curves. Fig. 4 presents the relative permeabilities curves employed for this case. We also compare the results obtained with the GPAS code using full tensor and corner point meshes, Marcondes et al. (2008). For this case, we have used three meshes: one is shown in Fig. 3b, the second is equivalent to the first one, but now rotated 45° counterclockwise, and the third one is a triangle mesh with 385 control volumes. The latter two mentioned meshes are shown in Fig. 5.

The last case study refers to a quarter-of-five spot, but now we have considered an isotropic and heterogeneous reservoir. Fig. 6 presents the porosity and absolute permeability field investigated. For this case we have used the quadrilateral mesh shown in Fig. 3b, the

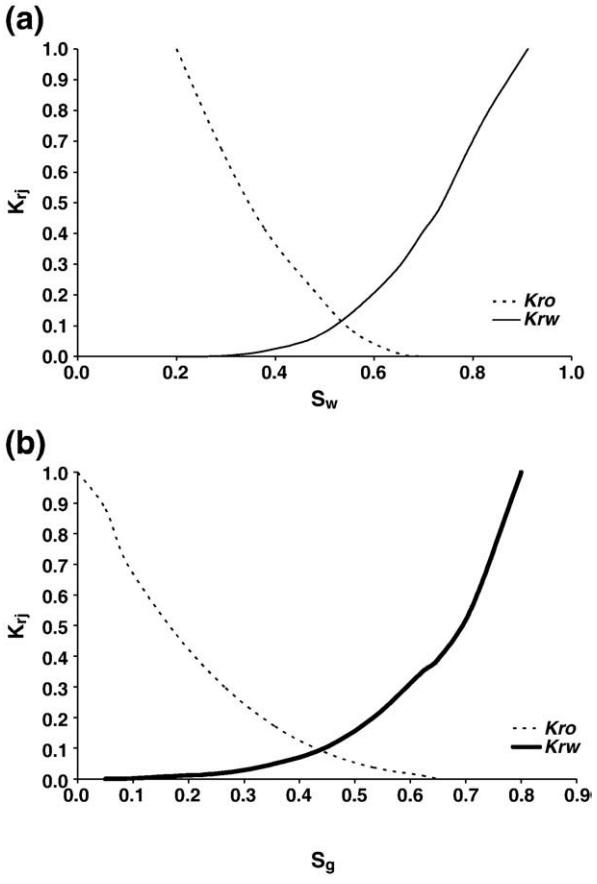

Fig. 4. Relative permeability curves.

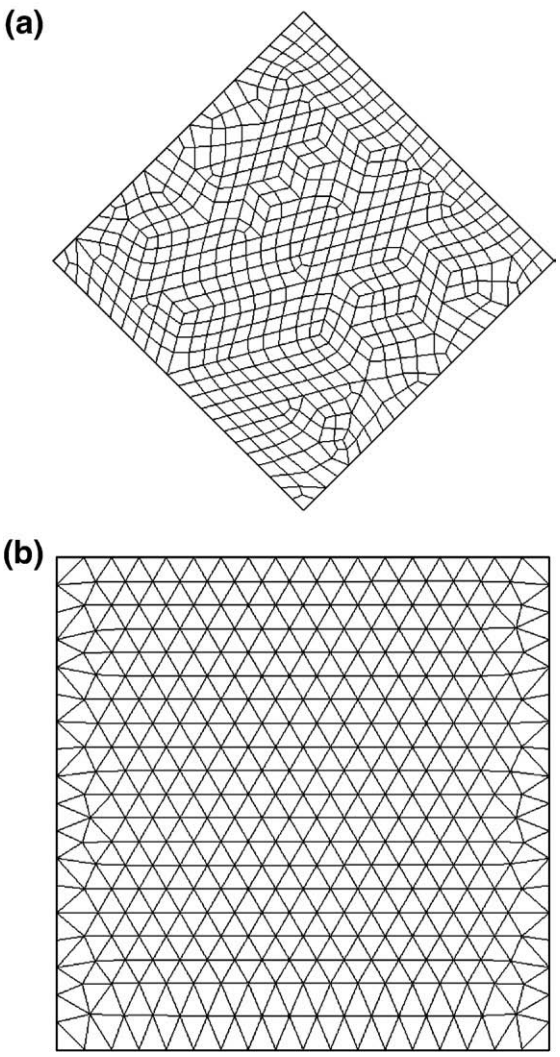

Fig. 5. Quadrilateral and triangular grid configurations used for case study 3. a) 619 control volumes and b) 385 control volumes.

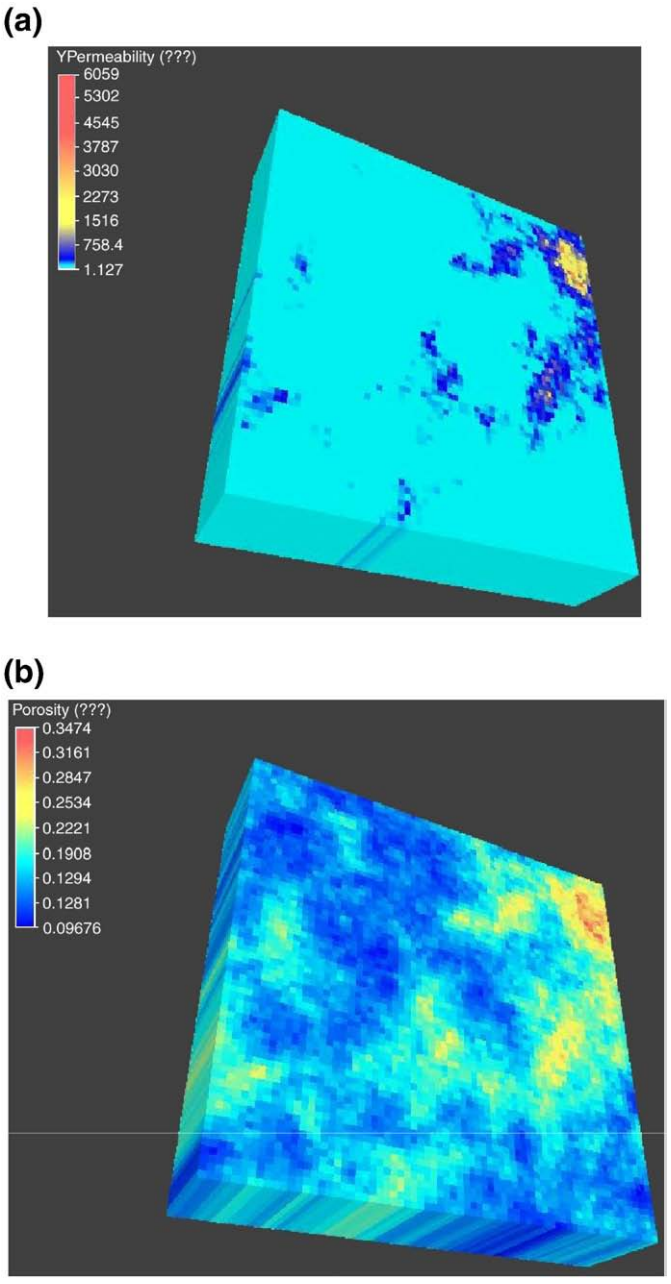

Fig. 6. Absolute permeability and porosity data used for case study 4.

triangle mesh shown in Fig. 5b, and two more refined quadrilateral meshes with 1173 and 1915 volumes. Except by the porosity and absolute permeability data set, the same parameters presented for case 3 were used in this case study.

5. Results

Fig. 7 presents the results in terms of volumetric rate at standard conditions for oil, and gas phases for case 1 using two-quadrangular meshes. The results of this simulation using the UTCOMP simulator in conjunction with Cartesian grids are also shown. Fig. 7 shows that the results of the present work using a coarse and a more refined quadrilateral mesh are very close for both oil and gas rates. Although the results obtained with UTCOMP simulator do not coincide with the ones obtained with the EbFVM, it can be inferred that when the mesh is refined using the UTCOMP simulator the results approach the ones using EbFVM. For a 120×120 Cartesian mesh the results for both oil and gas are in between the results using coarse and refined element-based method. To obtain a close result with Cartesian mesh it was necessary to use about 73 times more gridblocks compared to the coarse unstructured mesh whose results are very close to the ones obtained with the refined unstructured mesh.

The results in terms of volumetric rates of oil and gas rates at standard conditions obtained for case study 2 are shown in Fig. 8. The only difference between case studies 1 and 2 is the number of hydrocarbon components. For this case study, the reservoir fluid was characterized by 6 hydrocarbon components. Again, the results obtained in conjunction with the EbFVM for both coarse and refined meshes for oil and gas rates are very close to each other. Similarly, the results obtained with UTCOMP clearly approach the ones obtained using the EbFVM when the Cartesian mesh is refined. Mainly, the only difference when we compare the results obtained with traditional finite-volume method and EbFVM is the large number of control volumes necessary for the former approach to obtain approximately the same solution of the later mentioned approach.

The results for case study 3, the homogeneous anisotropic reservoir, in terms of volumetric rates at standard conditions of oil and gas obtained with two quadrilateral meshes and one triangular mesh are shown in Fig. 9. The results obtained with GPAS in

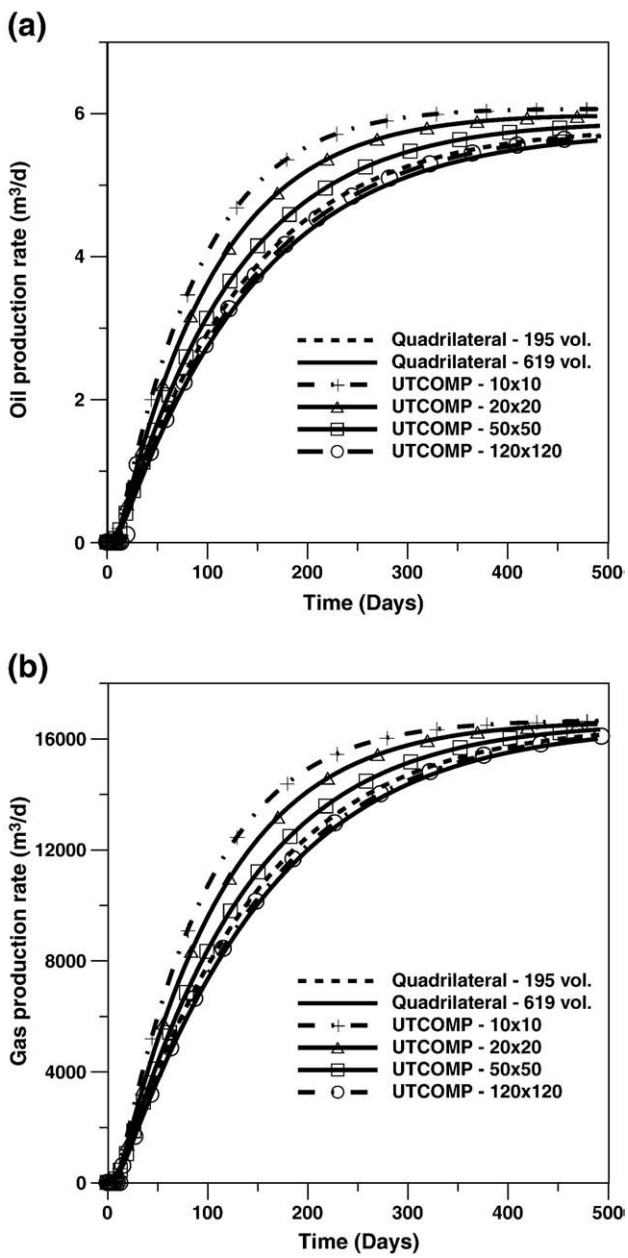

Fig. 7. Results for case 1. (a) Oil production rate vs. time and (b) gas production rate vs. time.

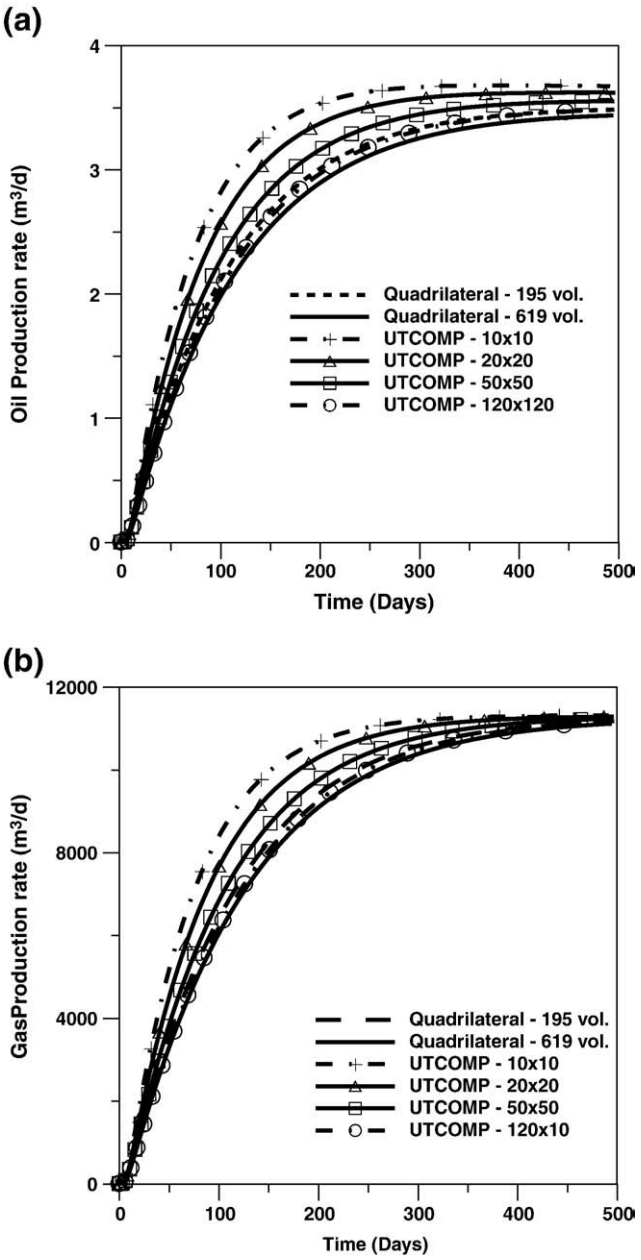

Fig. 8. Results for case 2. (a) Oil production rate vs. time and (b) gas production rate vs. time.

conjunction with Cartesian full tensor are also shown for two different meshes.

From Fig. 9, it can be seen that the results obtained using EbFVM for both quadrilateral and triangles give approximately the same solution. Also, the results for quadrilateral meshes present a small mesh orientation effect since the results with and without rotation are close to each other. Once again, if Cartesian meshes are employed it is necessary to use very refined meshes to obtain results close to the ones obtained with EbFVM approach.

Fig. 10 presents the results, in terms of oil and gas volumetric rates at standard condition, for the last case study. This figure shows that although some differences are observed between the results obtained using coarse and refined meshes, the differences are not significant. Also, the results with triangles and quadrilateral meshes were very similar, demonstrating the small grid orientation effect of the presented results.

6. Conclusions

An element-based finite-volume approach for compositional reservoir simulation using unstructured grids based on triangular and quadrilateral elements was presented. The results for the gas flooding simulation using triangular and quadrilateral elements were compared to the results obtained using an in-house simulator called UTCOMP in conjunction with Cartesian meshes. The results of UTCOMP using fine meshes were close to that ones obtained using the EbFVM approach implemented and tested in the present work. Grid orientation effects observed in the simulation results presented using EbFVM method were small. When these results were compared to the ones obtained using GPAS with full tensor Cartesian grids, it was observed that the simulation using Cartesian grids requires many more gridblocks than the EbFVM approach. For instance, the results obtained using quadrilateral and triangular elements with 619 and

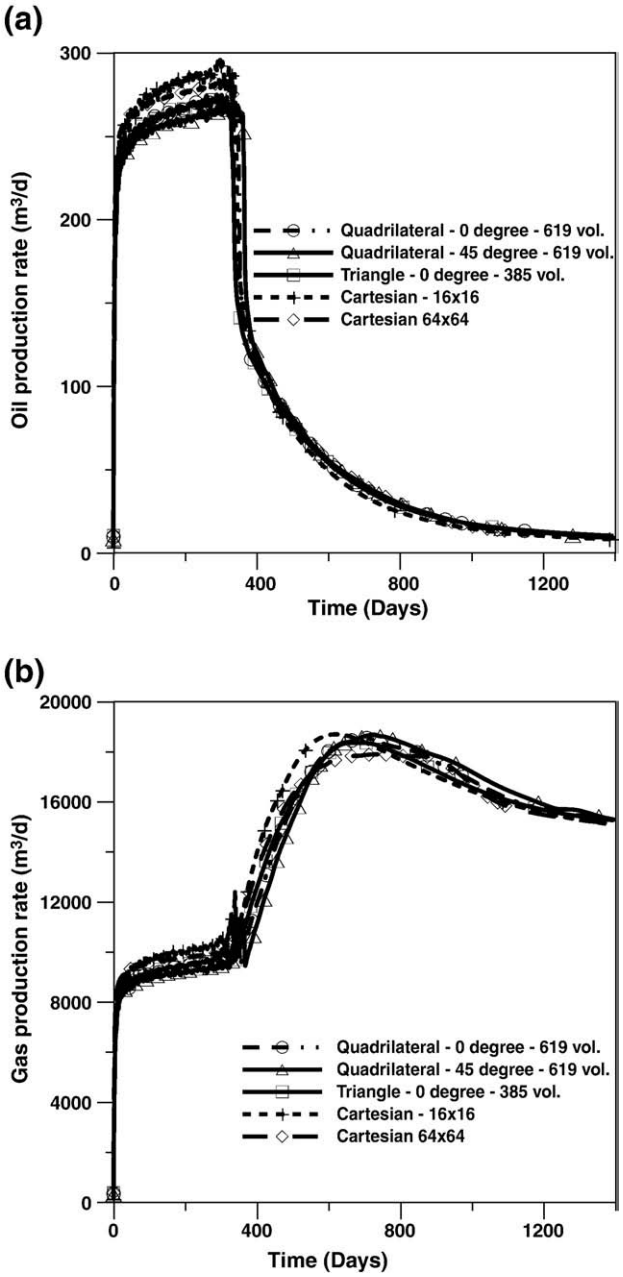

Fig. 9. Results for case 3. (a) Oil production rate vs. time and (b) gas production rate vs. time.

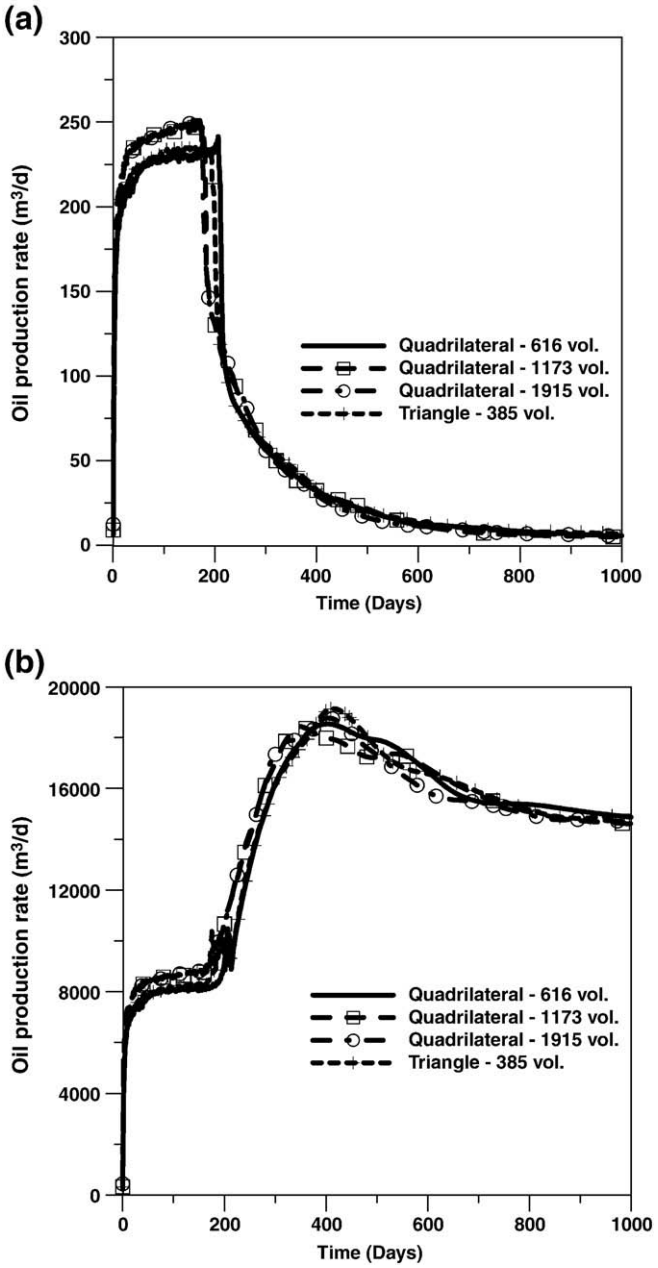

Fig. 10. Results for case 3. (a) Oil production rate vs. time and (b) gas production rate vs. time.

319 control volumes, respectively were very close. However, the results using a Cartesian 64×64 mesh (4096 gridblocks) were far from the previously mentioned results. In conclusion, the EbFVM approach was tested for several 2D case studies and based on the results the method seems to be an excellent method for solving such problems.

Acknowledgements

This work was conducted with the support of the Reservoir Simulation Joint Industry Project, a consortium of operating and service companies at the Center for Petroleum and Geosystems Engineering at The University of Texas at Austin. Also, the first author would like to thank CNPq (The National Council for Scientific and Technological Development of Brazil) for their financial support.

References

Baliga, B.R., Patankar, S.V., 1983. A control volume finite-element method for two-dimensional fluid flow and heat transfer. Numer. Heat Transfer 6, 245–261.

Chang, Y.B., Pope, G.A., Sepehrnoori, K., 1990. A higher-order finite difference compositional simulator. J. Petrol. Sci. Eng. 5 (1), 35–50.

Cordazzo, J., 2004. An Element Based Conservative Scheme using Unstructured Grids for Reservoir Simulation. SPE International Student Paper Contest, The SPE Annual Technical Conference and Exhibition, Houston, Texas.

Cordazzo, J., Maliska, C.R., Silva, A.F.C., Hurtado, F.S.V., 2004a. The Negative Transmissibility Issue When Using CVFEM in Petroleum Reservoir Simulation — 1. Theory. The 10th Brazilian Congress of Thermal Sciences and Engineering — ENCIT 2004, Braz. Soc. of Mechanical Sciences and Engineering — ABCM, Rio de Janeiro, Brazil, Nov. 29–Dec. 03.

Cordazzo, J., Maliska, C.R., Silva, A.F.C., Hurtado, F.S.V., 2004b. The Negative Transmissibility Issue When Using CVFEM in Petroleum Reservoir Simulation — 2. Results, The 10th Brazilian Congress of Thermal Sciences and Engineering — ENCIT 2004, Braz. Soc. of Mechanical Sciences and Engineering — ABCM, Rio de Janeiro, Brazil, Nov. 29–Dec. 03.

Deb, M.K., Reddy, M.P., Thuren, J.B., Adams, W.T., 1995. A New Generation Solution Adaptive Reservoir Simulator. Paper SPE 30720, The SPE Annual Technical Conference & Exhibition, Dallas, TX, October, 22–25.

Durlofsky, L.J., Chien, M.C.H., 1993. Development of a Mixed Finite-Element-Based Compositional Reservoir Simulator, Paper SPE 25253. The 12th SPE Symposium on Resevoir Simulation, New Orleans, LA, February 28–March 3.

Edwards, M.G., 2000. M-matrix flux splitting for general full tensor discretization operators on structured and unstructured grids. J. Comput. Phys. 160, 1–28.

Edwards, M.G., 2002. Unstructured, control-volume distributed, full-tensor finite-volume schemes with flow based grids. Comput. Geosci. 6, 433–452.

Forsyth, P.A., 1990. A Control-Volume, Finite-Element Method for Local Mesh Refinement in Thermal Reservoir Simulation, SPE paper 18415, (Nov.), pp. 561–566.

Fung, L.S., Hiebert, A.D., Nghiem, L., 1991. Reservoir Simulation with a Control-Volume Finite-Element Method, Paper SPE 21224. The 11th SPE Symposium on Reservoir Simulation, Anaheim, California, February 17–20.

Gottardi, G., Dall´Olio, D., 1992. A control-volume finite-element model for simulating oil–water reservoirs. J. Petrol. Sci. Eng. 8, 29–41.

Hegre, T.M., Dalen, V., Henriquez, A., 1986. Generalized Transmissibilities for Distorted Grids, Paper SPE 15622. The 61st Annual Technical Conference and Exhibition of the Society of Petroleum Engineers, New Orleans, LA. October 5–8.

Hoteit, H., Firoozabadi, A., 2005. Multicomponent fluid flow by discontinuous galerkin and mixed methods in unfractured and fractured media. Water Resour. Res. 41, 1–15.

Hoteit, H., Firoozabadi, A., 2006. Compositional modeling by the combined discontinuous Galerkin method and mixed methods. SPEJ 19–34.

Hughes, T.J.R., 1987. The Finite Element Method, Linear Static and Dynamic Finite Element Analysis. Prentice Hall, New Jersey.

Maliska, C.R., 2004, Heat Transfer and Computational Fluid Mechanics, Florianópolis, 2ª. Ed. Editora LTC. (In Portuguese).

Marcondes, F., Sepehrnoori, K., 2007. Unstructured Grids and an Element Based Conservative Approach for Compositional Reservoir Simulation. The 19th International Congress of Mechanical Engineering, November 5–9, Brasília, DF, Brazil.

Marcondes, F., Hang, C., Sepehrnoori, K., 2008. Effect of cross derivatives in discretization schemes in structured non-orthogonal meshes for compositional reservoir simulation. J. Petrol. Sci. Eng. 63, 53–60.

Parashar, M., Wheeler, J.A., Pope, G., Wang, K., Wang, P., 1997. A New Generation EOS Compositional Reservoir Simulator: Part II — Framework and Multiprocessing. Paper SPE 37977, SPE Reservoir Simulation Symposium, Dallas, USA.

Prévost, M., Edwards, M.G., Blunt, M.J., 2002. Streamline tracing on curvilinear structured and unstructured grids. SPEJ 7, 139–148.

Raw, M., 1985, A New Control Volume Based Finite Element Procedure for the Numerical Solution of the Fluid Flow and Scalar Transport Equations, Ph.D. Thesis, University of Waterloo, Waterloo, Ontario, Canada.

Verma, S., Aziz, K., 1997. A Control Volume Scheme for Flexible Grids in Reservoir Simulation. Paper SPE 37999, The Reservoir Symposium, Dallas, Texas, pp. 8–11.

Wang, P., Yotov, I., Wheeler, M., Arbogast, T., Dawson, C., Parashar, M., Sepehrnoori, K., 1997. A New Generation EOS Compositional Reservoir Simulator: Part I — Formulation and Discretization, Paper SPE 37079. SPE Reservoir Simulation Symposium, Dallas, Texas.